Innov Biosyst Bioeng, 2024, vol. 8, no. 4, 48–68
doi: 10.20535/ibb.2024.8.4.317985

Original article

CYTODESTRUCTIVE EFFECTS OF PHOTODYNAMIC EXPOSURE IN PRIMARY CULTURES OF MALIGNANT GLIOMA CELLS

V.D. Rozumenko[1], L.D. Liubich[2*], L.P. Staino[2], D.M. Egorova[2], A.V. Dashchakovsky[1], T.A. Malysheva[3]

[1]Department of innovative neurosurgical technologies, department of neurooncology and pediatric neurosurgery, State institution "Romodanov Neurosurgery Institute, National Academy of Medical Sciences of Ukraine", Kyiv, Ukraine
[2]Tissue culture laboratory, department of neuropathomorphology, State institution "Romodanov Neurosurgery Institute, National Academy of Medical Sciences of Ukraine", Kyiv, Ukraine
[3]Pathological-anatomical laboratory, department of neuropathomorphology, State institution "Romodanov Neurosurgery Institute, National Academy of Medical Sciences of Ukraine", Kyiv, Ukraine

*Corresponding author: lyubichld@gmail.com

Received 1 October 2024; Accepted 1 December 2024

Background. Photodynamic therapy (PDT) is a promising adjuvant method for the treatment of malignant gliomas (MG), including tumors with continued growth and tumor recurrences. For the clinical application of PDT, it is important to substantiate the effectiveness of the cytodestructive effect of the combined use of laser irradiation (LI) and photosensitizer (PS).

Objective. To evaluate the cytodestructive effects of photodynamic exposure with the use of PS chlorine E6 on primary MG cell cultures.

Methods. Primary cell cultures were obtained from samples of biopsy material from patients (n = 6) with a verified diagnosis: 3 primary tumors (1 case of diffuse astrocytoma, NOS (G3), 1 – glioblastoma (GB), NOS (G4), 1 – gliosarcoma (G4)) and 3 – with continued tumor growth (1 – diffuse astrocytoma, NOS (G3), 1 – oligodendroglioma, NOS (G3) and 1 – GB, NOS (G4). Groups of cell cultures included: 1) control – cultured in a standard nutrient medium and experimental; 2) cultured with the addition of chlorine E6 (2.0 μg/ml); 3) cultivated without the addition of PS and subjected to LI; 4) cultivated with the addition of chlorine E6 and subsequent exposure to LI. After 24 h, morphological and morphometric studies were carried out.

Results. The primary MG cultures were characterized by different growth dynamics; mitotic activity of tumor cells varied from the highest rate in the culture of primary GB to lower values – in cultures of recurrent GB and primary astrocytoma and gliosarcoma, and the lowest – in cultures of continued growth of astrocytoma and oligodendroglioma after combined treatment. Direct exposure to chlorine E6 and LI reduced the total number of cells in the culture and their mitotic activity. The greatest cytodestructive effect was achieved with the combined effect of chlorine E6 and LI: the effective dose in the case of primary astrocytoma cells is 10 J/cm^2 in pulse mode; for cells of primary GB and gliosarcoma, recurrent astrocytoma and oligodendroglioma, the effective dose is 25 J/cm^2 in pulsed mode. In the case of GB cells, continued growth, a dose of 25 J/cm^2 is effective for both continuous and pulsed modes of LI.

Conclusions. Primary cell cultures of MG obtained directly from tumor tissue are an adequate model for evaluating the effectiveness of the cytodestructive effect of the combined use of LI and PS for PDT.

Keywords: malignant glioma; continued growth; primary cultures; photodynamic therapy; chlorine E6; laser irradiation, mitotic index.

Introduction

According to the National Cancer Registry, the incidence of malignant variants of primary brain tumors in Ukraine is 4.8% per 100,000 population, and the mortality rate is 3.5% [1]. Gliomas are conditionally divided into two large groups [2]: circumscribed gliomas, which have relatively well-defined borders and can be completely removed surgically, and diffuse gliomas, which do not have clear borders and cannot be totally removed during surgery. According to the new edition (2021) of the classification of tumors of the central nervous system (CNS), in adults diffuse gliomas are divided into three groups: astrocytomas (CNS WHO grade 2–4), oligodendrogliomas (CNS WHO grade 2, 3), glioblastomas (GB, CNS WHO grade 4) [3]. It is diffuse gliomas that are the most malignant gliomas (MG) of the brain (WHO grade 3, 4), have a significantly worse prognosis in terms of duration of overall and recurrence-free survival [2], prevail among primary tumors of the CNS, most of them are GB [4].

The modern standard of treatment in the course of MG is surgical treatment with maximum functionally possible resection, radiochemotherapy, and adjuvant chemotherapy [5]. However, with advances in neurosurgery, chemotherapy, and radiation therapy, MG remain one of the most treatment-

resistant CNS malignancies, and the tumor inevitably progresses. When using traditional surgical approaches and imaging methods when removing a diffuse glioma, tumor cell infiltrates in the zone of invasion may be overlooked, as a result of which prolonged growths/recurrences of MG often occurs near the edge of the surgical cavity [6].

Many new treatment methods are designed to combat these local recurrences by injecting therapeutic agents directly into or near the tumor bed. Photodynamic methods, such as photodynamic diagnostics, tumor resection under fluorescence control (fluorescence-guided surgery (FGS)) and photodynamic therapy (PDT) are used as adjuvant therapy methods for brain MG, with the aim of visual intraoperative identification of tumor tissue and its simultaneous selective destruction [7, 8]. PDT involves the introduction of a light-sensitive chemical agent (photosensitizer (PS)) followed by its activation at a certain wavelength of light to achieve cytotoxic effects in malignant tumor cells [9–12].

According to the available information on clinical trials, the use of PDT as an additional method of MG treatment immediately after maximum resection is safe, reduces the risk of recurrence due to the targeted destruction of residual tumor cells in the resection cavity, improves survival and quality of life of patients [7, 13–19]. In addition, the use of PDT is promising for local recurrences of MG [15, 17].

PDT is an effective alternative to traditional approaches in the treatment of malignant neoplasms; can be used both independently and in schemes of combined and complex therapy. Significant advantages of PDT are relatively less invasiveness due to the preferential targeting of tumor cells incorporating PS for their destruction due to the cytotoxic effect of the products of the photodynamic reaction; slight toxicity for normal tissues surrounding the tumor; minimal risk of severe pain syndrome; lack of primary and acquired resistance mechanisms; possibility of outpatient treatment and combination with other methods of treatment; absence of limiting cumulative doses of PS and laser irradiation (LI); ease of use with multiple lesions; the possibility of implementing organ-preserving treatment methods [20–22]. The search for new PSs with greater tissue specificity and modifications of already available PSs in order to minimize their impact on individual organs and eliminate the potentially harmful effect of PDT on healthy tissues continues.

Chlorine E6, natural pigment from green algae (molecular formula $C_{34}H_{36}N_4O_6$) [23], is one of the most effective PS currently used in PDT [24]. Its advantages are low toxicity, rapid dissolution and removal from the body, absence of dark toxicity, as well as strong fluorescence [10, 25], antibacterial, anti-inflammatory and antimicrobial properties [26]. The disadvantages of chlorine E6 are its hydrophobicity, and as a result – ineffective pharmacokinetics, poor biodistribution and limited penetration depth [27]. To acquire water solubility, chlorine E6 is conjugated with polyvinylpyrrolidone (a biocompatible polymer), which promotes accumulation in the tumor due to increased permeability of defective tumor vessels and weakened lymphatic drainage [28].

For the clinical application of photodynamic exposure technologies, the personalized selection of optimal doses of LI and PS is relevant and appropriate for evaluating the effectiveness of PDT schemes, which requires preliminary preclinical studies on primary cell cultures of MG obtained directly from tumor tissue.

Objective: to evaluate the effects of photodynamic exposure using the photosensitizer chlorine E6 on primary cultures of malignant glioma cells.

Materials and Methods

The study was carried out on primary cultures of human MG cells, obtained from samples of biopsy material from patients (n = 6), who were undergoing examination and treatment at the State Institution "Romodanov Neurosurgery Institute, National Academy of Medical Sciences of Ukraine" (SI "INS NAMS") and provided informed consent. The tumor diagnosis was verified by histological examination: 3 primary MG (1 case of diffuse astrocytoma, NOS (not otherwise specified) (CNS WHO grade G3), 1 case of GB, NOS (CNS WHO grade G4), 1 case of gliosarcoma (CNS WHO grade G4) and 3 – with continued growth (1 case of diffuse astrocytoma, NOS (CNS WHO grade G3), 1 case of oligodendroglioma, NOS (CNS WHO grade G3) and 1 case of GB, NOS (CNS WHO grade G4), according to the WHO approved updated version of the classification of CNS tumors (2021) [3]. Clinical parameters of the patient cohort are shown in the Table.

The study was conducted within the framework of scientific research work (state registration No. 0122U000331) in accordance with the protocol agreed by the Committee on Bioethics of the SI "INS NAMS" (protocol No. 2 dated 04/14/2021) and in accordance with the principles of bioethics, established by domestic and international legislation.

Table: Clinical parameters of the patient cohort

Patient	Sex	Age (years)	Diagnosis	ICD-O-3 histopathology and behavior code	Grading	Primary/recurrent
1	f	42	Diffuse astrocytoma, NOS	9401/3	G3	Primary
2	m	62	Glioblastoma, NOS	9440/3	G4	Primary
3	m	59	Gliosarcoma	9442/3	G4	Primary
4	m	38	Diffuse astrocytoma, NOS	9401/3	G3	Recurrent
5	m	56	Oligodendroglioma, NOS	9442/3	G3	Recurrent
6	f	51	Glioblastoma, NOS	9440/3	G4	Recurrent

Note. NOS – not otherwise specified.

Cell suspensions were obtained from samples of biopsy material, 10 ml of MEM medium with L-glutamine without serum (Biowest, France) was added and centrifuged (5 min at 1000 rpm, MICROmed CM-3), the cell sediment was suspended in MEM medium with L-glutamine, 1 mmol of sodium pyruvate, 10% fetal calf serum (FCS, "Biowest", France) and in the amount of $2 \cdot 10^6$/2 ml of the medium were transferred to plastic Petri dishes ($d = 35$ mm, Sarstedt, Germany) on coverslips slides pre-coated with polyethylenimine (Sigma-Aldrich, GmbH, Germany) and cultured until reaching a monolayer (75–80%).

Cultures were kept in a CO_2 incubator (Nuve, Turkey) under standard conditions (95% humidity, 37 °C, 5% CO_2). The nutrient medium was changed every three days. Dynamic observation with microphotographic registration was performed on a Nikon S-100 inverted microscope (Japan).

To study the direct effects of PS, chlorine E6 (2 μg/ml) was added to cell cultures with a formed monolayer. To study the direct effects of LI, dishes with cell cultures were placed under the vertical fiber optic laser output (h = 5 cm) of the device "LIKA-surgeon" ("Fotonika-Plus", Ukraine) and exposed to irradiation with uniform coverage of the monolayer area by light rays (λ – 660 nm) in different modes (power 0.6 W, dose – 10–25 J/cm^2, continuous or pulse mode). The exposure time of LI to the cell culture depended on the applied dose and mode (the minimum duration of irradiation was 17 s for LI 0.6 W, 10 J/cm^2, continuous mode, the maximum – 80 s for LI 0.6 W, 25 J/cm^2, pulse mode). The irradiated cultures were kept at room temperature during this time, while the cultures of the comparison groups were kept under similar conditions.

To study the combined effect of chlorine E6 and LI, PS (2 μg/ml) was added to cell cultures with a formed monolayer and they were kept in a CO_2-incubator (Nuve, Turkey) for 4 h, after which the cultures were exposed to irradiation under different regimes as indicated above.

After exposure to the specified experimental factors, the cultures were kept in a CO_2 incubator and dynamic observation was carried out with microphotographic registration on a Nikon S-100 inverted microscope for 24 h. Microphotographic recording of fluorescence was performed on an Axiophot microscope (OPTON, Germany) using fluorescent filters (range λ = [500–680] nm).

To determine the cytotoxic effect of chlorine E6 and LI, cell cultures were exposed to various experimental conditions with the addition of a vital dye (0.2% trypan blue (TB) solution (Merck, Germany)) to the culture medium, and culture growth was observed under an inverted microscope for 24 h.

For further analysis, groups of cell cultures were formed depending on the conditions of cultivation and exogenous influence (Fig. 1): 1) control – cultivated in a standard nutrient medium (MEM with L-glutamine, 1 mmol of sodium pyruvate, 10% FCS) and experimental: 2) cultured under conditions of addition of chlorine E6 (2.0 μg/ml); 3) cultured on a nutrient medium without the addition of PS and subjected to LI (power 0.6 W, dose 10–25 J/cm^2, continuous or pulse mode); 4) cultured under conditions of addition of chlorine E6 and subsequent exposure to LI (power 0.6 W, dose 10–25 J/cm^2, continuous or pulse mode). Each variant of the experimental effect was studied in 3 repetitions. The LI dose range and PS concentration were selected in previous experiments on human GB cell cultures of the U251 line [29].

Cell cultures were fixed in 10% neutral formalin (Bio-Optica, Italy) and stained with hematoxylin-eosin according to Carazzi. Microscopic exa-

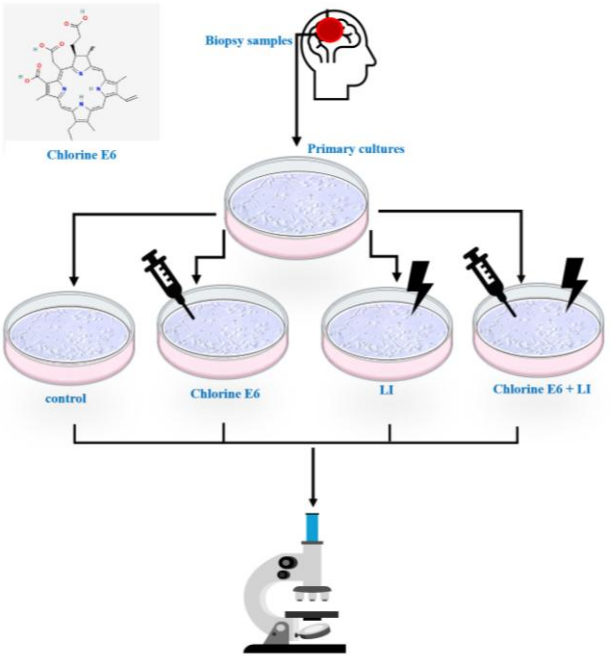

Figure 1: Scheme of experimental study (LI – laser irradiation)

mination and photo-registration of cytological preparations of cultures was carried out using a light-optical photomicroscope NIKON Eclipse E200 (Japan). In each preparation, the features of the structure of the experimental cultures compared to the control ones, the shape of the cells, the presence and branching of processes, the structure and nature of the distribution of chromatin and the shape of the nuclei, the features of intercellular interactions were analyzed.

Quantitative studies of control and experimental cultures were carried out in 10 representative fields of view with a standard measuring scale (object – micrometer). Morphometric analysis was carried out by processing digital images of cultures in 10 arbitrarily selected fields of view (0.04 mm^2) for each sample at the same magnification (800×) using ImageView software (2020), determining on the test area the number of viable cells, the total number of cells, the number of cells in the state of mitotic division. The mitotic index (MI, %) was calculated as the proportion of cells with the presence of mitoses per 100 cells.

Statistical analysis of the obtained data was performed using StatSoft Inc. software (2022). Non-parametric methods of variational statistics were applied (Kruskel-Wallis ANOVA rank discriminant analysis for multiple comparison of several independent groups, Mann–Whitney U-test for pairwise comparison of independent groups). The normality of data distribution was determined by the Shapiro–Wilk test. The data are presented in the form (M ± m), where M is the average value; m is the standard deviation from the mean value. Differences at $p < 0.05$ were considered statistically significant.

Results

The effects of photodynamic exposure to chlorine E6 in primary MG cell cultures.

Primary MG cell cultures (control) were characterized by unequal growth dynamics, forming a confluent monolayer from the 18th to the 25th day, depending on the individual characteristics of the tumor. Vital dye TB was accumulated only in spontaneously degenerated round cells with reduced appendages (Figs. 2–7, A). Cells had spontaneous fluorescence of pale blue color, incorporation of chlorine E6 caused fluorescence of bright pink-crimson color (when using fluorescent filters in the range $\lambda = [500–680]$ nm, Figs. 2–7, B). Histological examination made it possible to characterize in detail the morphological features of cultured cells (Figs. 2–7, C).

Astrocytoma cell cultures (CNS WHO grade G3). Control cultures reached confluent growth on the 25th day: the monolayer formed large cells with clear contours, distinct cytoplasm, a large light nucleus, unipolar, triangular, rhomboid, polygonal in shape with short appendages with branches (Fig. 2A). In sparser areas of the growth zone, intercellular connections were formed with the formation of reticular architecture. Cell nuclei had moderate atypia (Fig. 2C). Single cells in the stages of mitotic division were noted (MI was (0.27 ± 0.01) % (Fig. 8A).

After 24 h of incubation with chlorine E6, areas with destruction of the monolayer architecture were detected, with single isolated cells between fragments of dead cells; the integrity of membranes was preserved in most cells (Fig. 2A). Chlorine E6 was incorporated into the cytoplasm and perinuclear space of tumor cells (Fig. 2B). Most of the cells had structural features of dystrophic changes (Fig. 2C): condensed and reduced cytoplasm, shrunken and pyknotic nuclei; cells without clear contours had large unevenly thinned cytoplasm with numerous pinocytic bubbles and vesicles, perinuclear emptying and decentralized atypical nuclei with heavy chromatin condensation. Against the background of a general decrease of cells in the culture ($p = 0.01$ compared to the control, Mann–Whitney U-test), no cells in a state of mitotic division were detected (Fig. 8A).

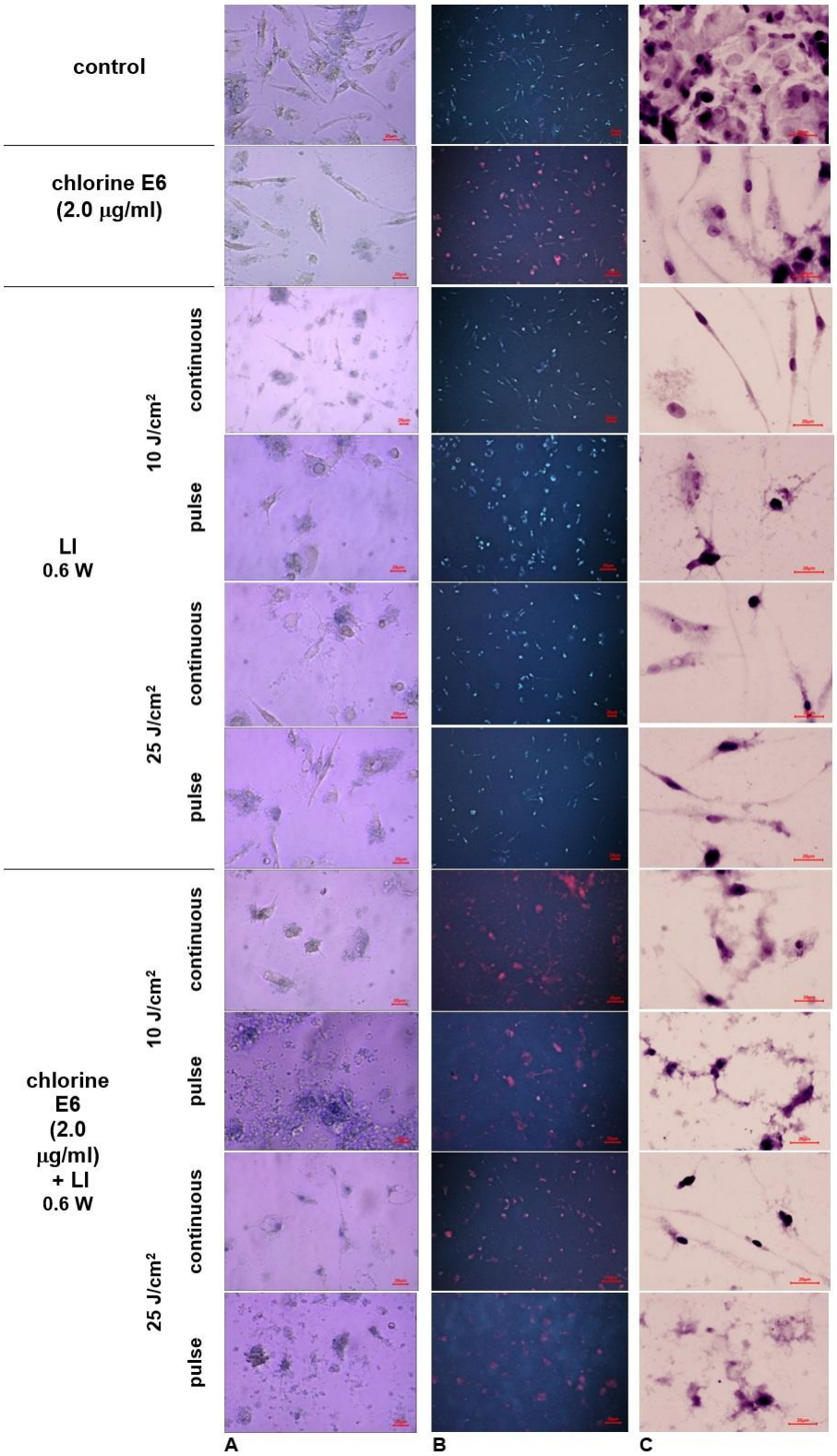

Figure 2: Photomicrograph of human astrocytoma (G3) cell cultures under the influence of chlorine E6 (2 μg/ml) and laser irradiation in different modes. Light (A, C) and fluorescence (B) microscopy, staining with vital dye trypan blue (A) and hematoxylin-eosin (C). Scale 20 μm

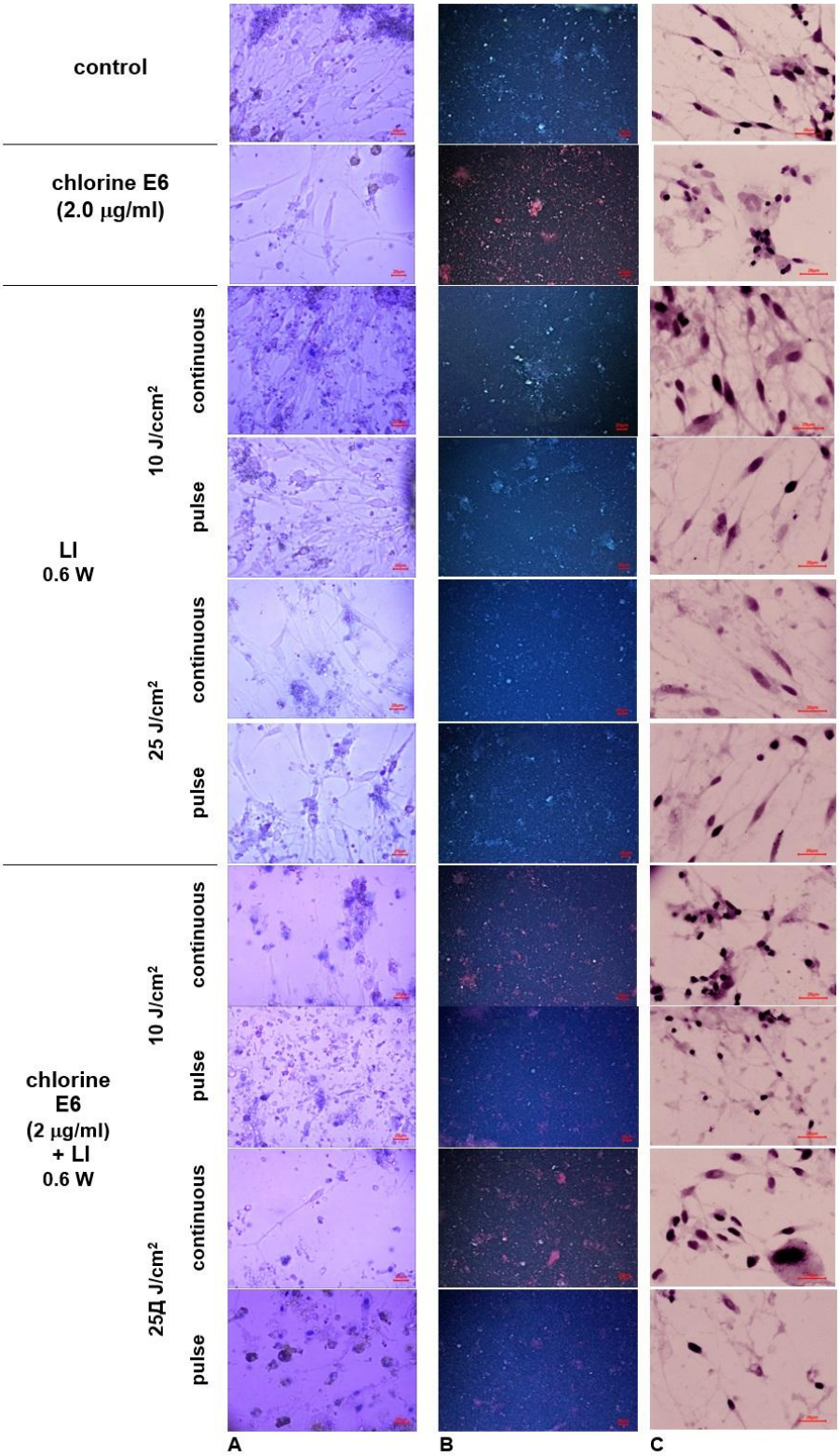

Figure 3: Photomicrograph of human glioblastoma (G4) cell cultures under the influence of chlorine E6 (2 μg/ml) and laser irradiation in different modes. Light (A, C) and fluorescence (B) microscopy, staining with vital dye trypan blue (A) and hematoxylin-eosin (C). Scale 20 μm

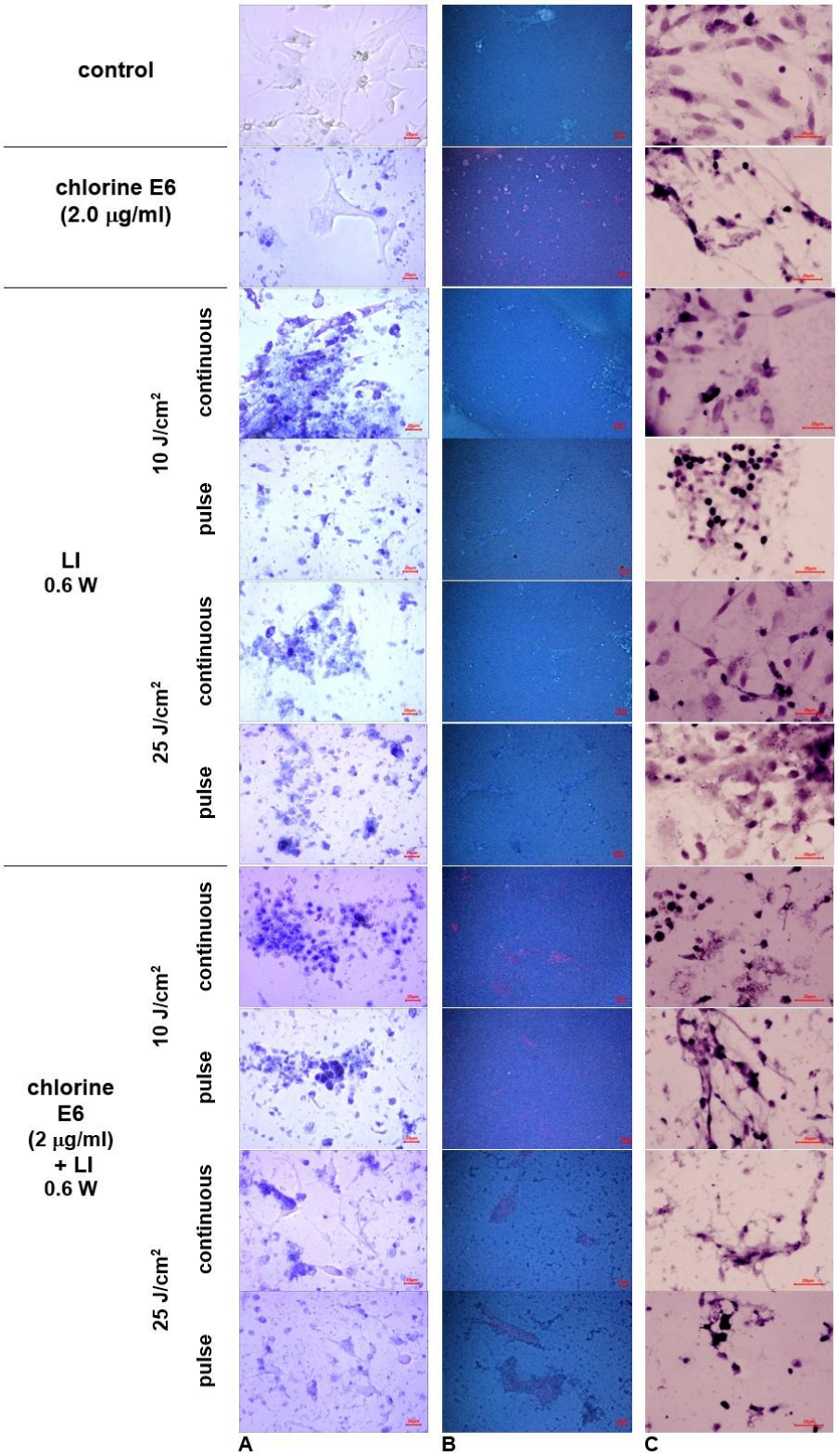

Figure 4: Photomicrograph of human gliosarcoma (G4) cell cultures under the influence of chlorine E6 (2 μg/ml) and laser irradiation in different modes. Light (A, C) and fluorescence (B) microscopy, staining with vital dye trypan blue (A) and hematoxylin-eosin (C). Scale 20 μm

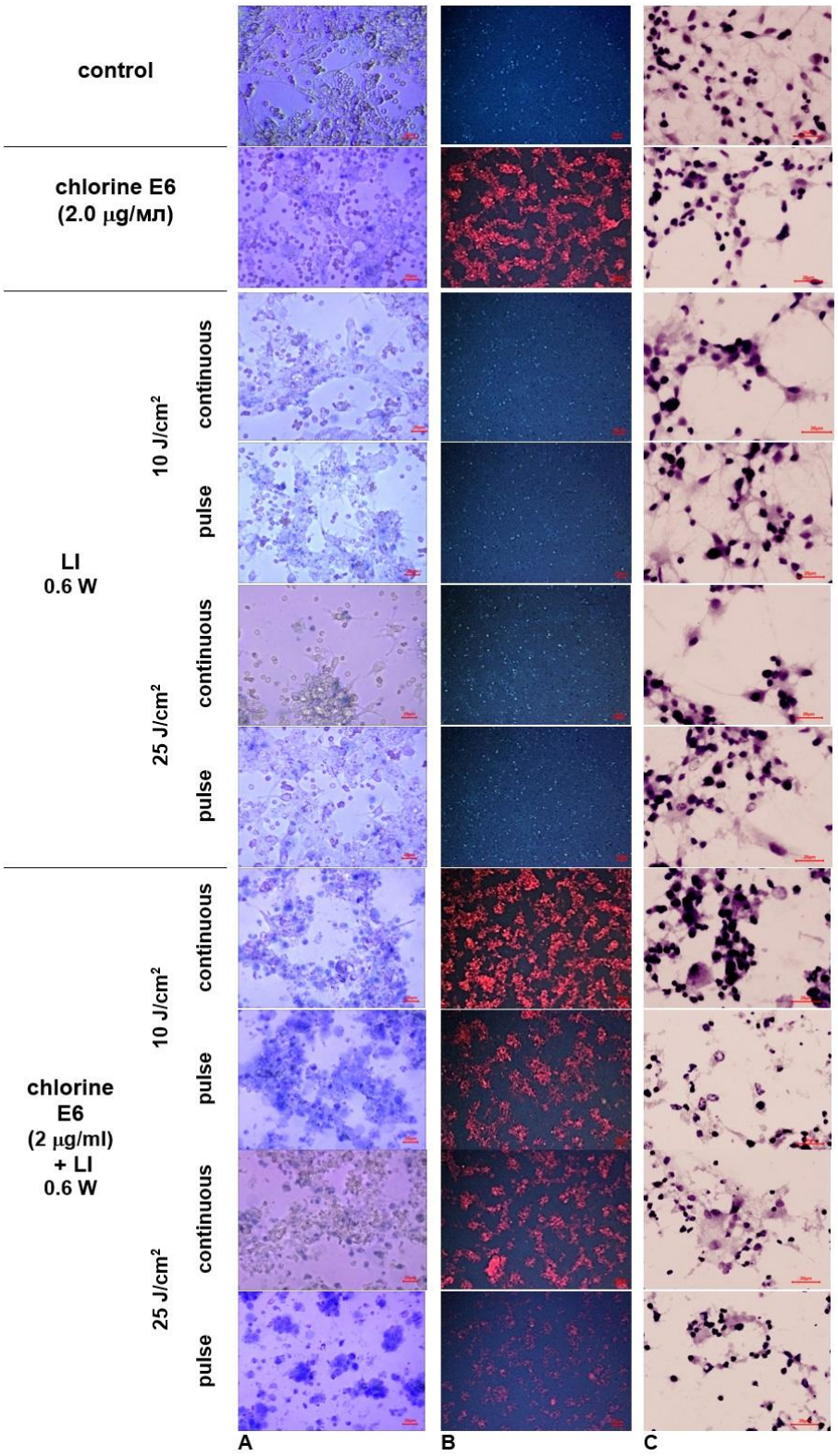

Figure 5: Photomicrograph of human astrocytoma (G3, continued growth) cell cultures under the influence of chlorine E6 (2 μg/ml) and laser irradiation in different modes. Light (A, C) and fluorescence (B) microscopy, staining with vital dye trypan blue (A) and hematoxylin-eosin (C). Scale 20 μm

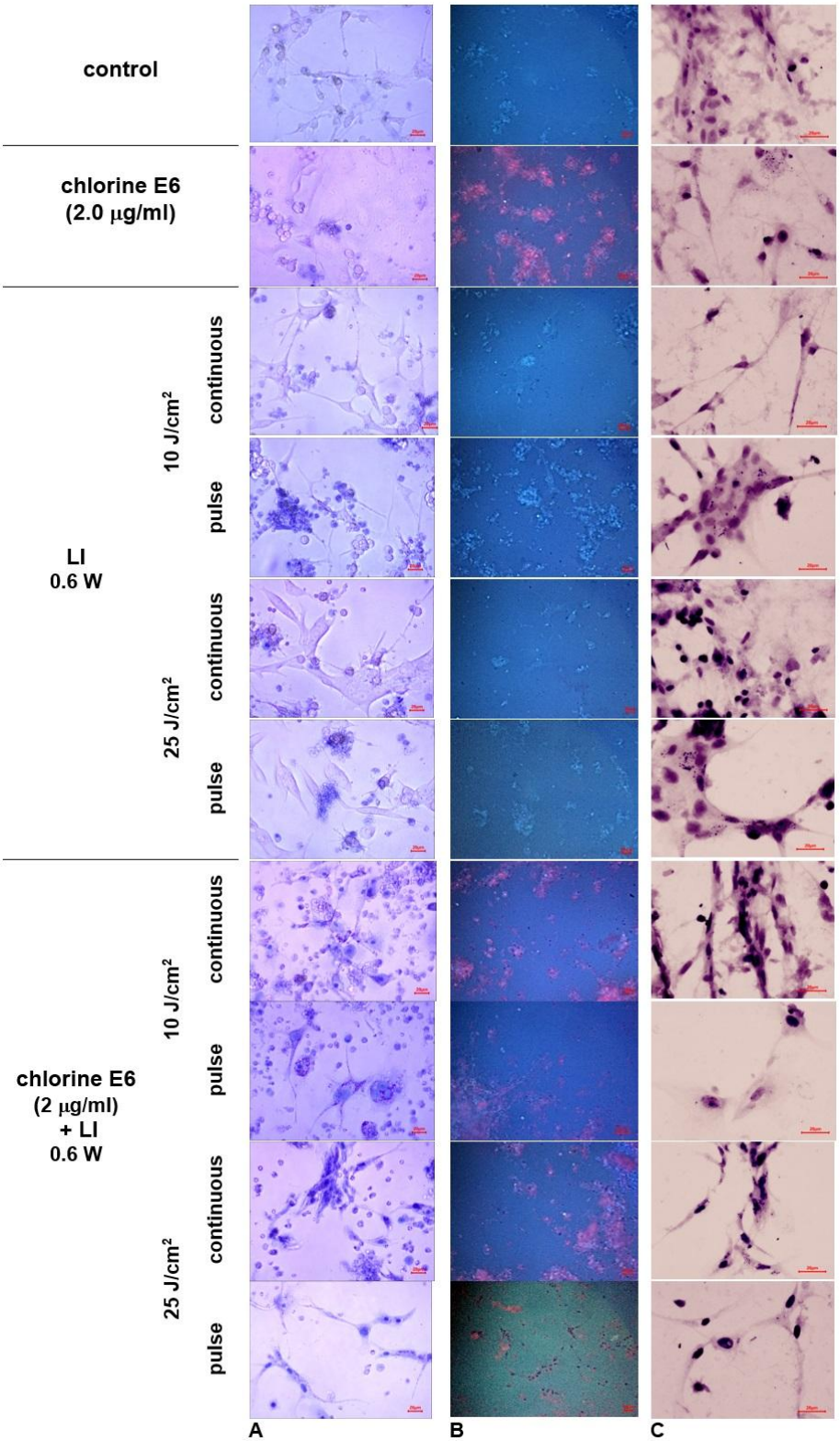

Figure 6: Photomicrograph of oligodendroglioma (G3, continued growth) cell cultures under the influence of chlorine E6 (2 μg/ml) and laser irradiation in different modes. Light (A, C) and fluorescence (B) microscopy, staining with vital dye trypan blue (A) and hematoxylin-eosin (C). Scale 20 μm

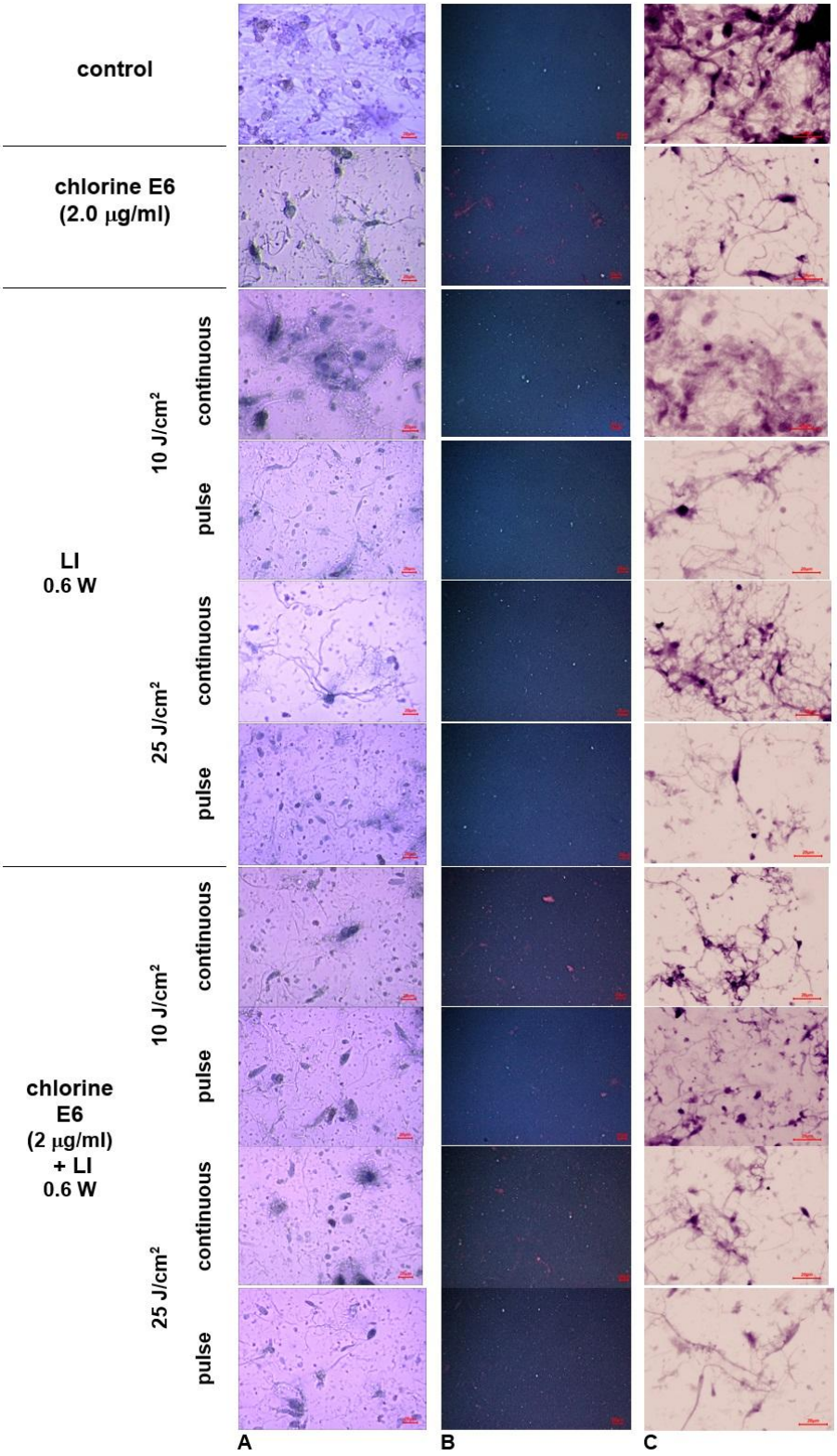

Figure 7: Photomicrograph of glioblastoma (G4, continuous growth) cell cultures under the influence of chlorine E6 (2 μg/ml) and laser irradiation in different modes. Light (A, C) and fluorescence (B) microscopy, staining with vital dye trypan blue (A) and hematoxylin-eosin (C). Scale 20 μm

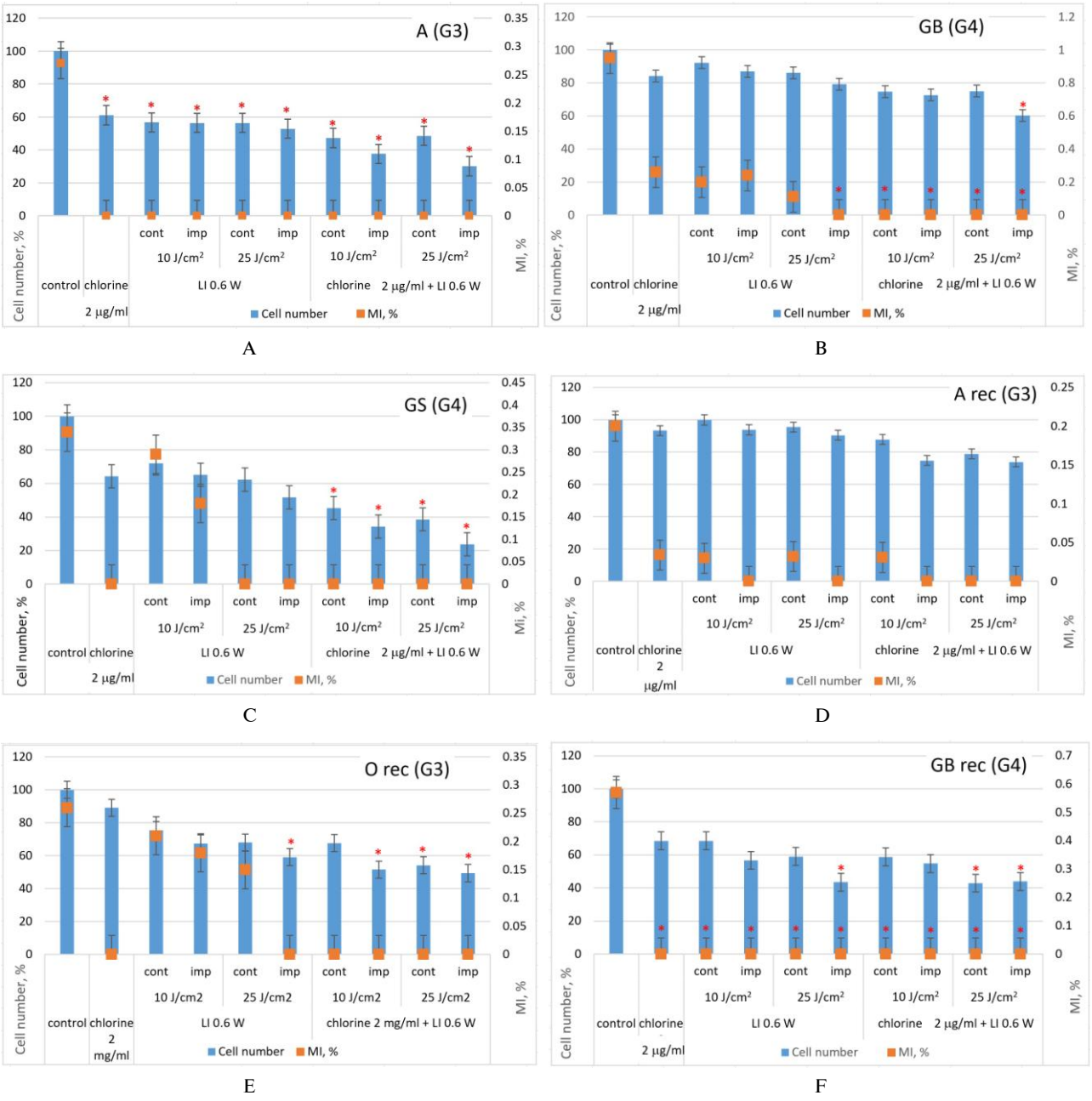

Figure 8: Indicators of the average number (%) of cells and the mitotic index (MI, %) in the cultures of human MG cells under the influence of chlorine E6 (2 μg/ml) and laser irradiation in different modes: (A) A – astrocytoma; (B) GB – glioblastoma; (C) GS – gliosarcoma; (D) A rec – astrocytoma, continued growth (recurrence); (E) O rec – oligodendroglioma, continued growth (recurrence); (F) GB rec – glioblastoma, continued growth (recurrence); * – $p < 0.05$, compared to the control, Mann–Whitney U-test

Under direct exposure to LI 10 J/cm² in continuous mode, a significant thinning of the growth zone was observed in cell cultures, in some areas – loss of intercellular adhesion, degenerated cells with reduced processes and rounded cytoplasm. Cell membranes were damaged (Fig. 2A), the cytoplasm of some cells were condensed, the nuclei were elongated or flattened, reduced in size, in a state of karyopyknosis; in other cells – abrasion of membranes, a large number of vacuoles and perinuclear devastation, nuclei in a state of pyknosis were observed (Fig. 2C). Under the same conditions, the pulse mode of LI led to a significant thinning of the growth zone, a violation of the integrity of membranes (TB grains in the cytoplasm of cells). Among the cells with a preserved form with short,

branched processes, cells with homogenization and reduction of the cytoplasm, the formation of "ghost" cells with pyknotic nuclei, loss of clarity of the optical boundaries of cells, perinuclear devastation and distinct vacuolar degeneration, pyknosis and karyorrhexis of nuclei were found.

With an increase in the LI dose to 25 J/cm^2 in a continuous mode, further thinning of the growth zone, multinucleated cell forms, and accumulation of TB in the form of grains in the cytoplasm were observed. Pathomorphological changes of cells included: vacuolization of the cytoplasm, violation of the integrity of the plasmalemma, hydropic dystrophy, shift of the nucleus to the periphery, sometimes its vacuolization or shrinkage, protrusions and marginality of chromatin along the karyolemma; appearance of anucleate cells. Under the influence of LI in the pulse mode, the destruction of the growth zone and disintegration into individual cells with loss of intercellular contacts, degenerative – dystrophic changes in cells were observed: cytoplasm compaction, cell and appendages size reduction, vacuolization, destruction of membranes; nuclei in a state of pyknosis, with perinuclear devastation, shrunken or with deep condensation of chromatin (Fig. 2, A, C).

Under the combined effect of chlorine E6 and LI 10 J/cm^2 in a continuous mode against the background of the devastated growth zone, local large intact areas of the monolayer formed by cells with preserved morphology were detected. The rest of the cells underwent significant changes: reduction of processes, condensation of the cytoplasm, vacuoles in the perikaryon, the so-called "ring-shaped" cells; nuclei of an atypical shape, hyperchromic, with protrusions or in a state of karyopyknosis. Under the same conditions, in the pulse mode, the death of most cells and individual cells of bipolar form, gradual densification of the cytoplasm of cells with a marked increase in its homogeneity; cell nuclei in a state of karyopyknosis and karyolysis; anucleate cells were observed (Fig. 2, A, C).

Under the combined effect of chlorine E6 and a higher dose of LI 25 J/cm^2 in a continuous mode, complete destruction of the growth zone, isolated clusters of cells with loss of contacts, rounded (with complete or partial reduction of processes) and elongated spindle-like cells, which accumulated TB both in the cytoplasm and in the nucleus were observed (Fig. 2A). Huge vacuoles turned some of the cells into "shadow" cells. Some of the cells, with compacted or completely reduced cytoplasm, were in a state of pyknosis; "ghost" cells with perinuclear vacuolization and pyknotic nuclei, cytoplasmic drying and distinct vacuolar degeneration were observed. Under the same conditions in pulse mode, total degeneration of cells and their sequestration, "bare" nuclei and "shadow" cells were observed (Fig. 2C).

According to quantitative studies, against the background of a gradual general decrease of cells in the astrocytoma culture under the influence of experimental factors, starting with incubation with chlorine E6, cells in a state of mitotic division were not detected ($p = 0.01$ compared to the control, Mann–Whitney U-test; Fig. 8A). In the process of changing the experimental factors from direct exposure to chlorine E6 or LI to their combined influence, there was a gradual increase in cytodestructive effects in the culture of astrocytoma cells, reaching a subtotal character already under the conditions of combined exposure to chlorine E6 and a lower dose of LI 10 J/cm^2 in pulse mode (under these conditions, the number of cells in the culture decreased by 2.6 times ($p = 0.006$ compared to the control, Mann–Whitney U-test, no mitotic activity was detected).

GB (CNS WHO grade G4) cell cultures. Control cell cultures reached confluent growth on the 16th day: massive reticular growths of different morphological cell types (spindle-like, fibroblast-like, triangular and star-like, with long branched processes) formed a network (Fig. 3A). MI was $(0.95 \pm 0.09)\%$ (Fig. 8B), significantly exceeding the indicator of astrocytoma cells ($p = 0.03$, Mann–Whitney U-test).

After 24 h of incubation with chlorine E6, the growth zone was destroyed, most of the cells were necrotic, small, rounded in shape, with varying degrees of process reduction. In small fragments of the growth zone, cells with appendages (Fig. 3A), vacuolar dystrophy and pyknotic nuclei with perinuclear devastation (Fig. 3C); cells of giant forms with vacuolated nuclei, destroyed plasmalemma and compaction of the cytoplasm or its complete reduction; karyolysis, "shadow" and anucleate cells were detected. MI decreased to $(0.26 \pm 0.08)\%$ ($p = 0.25$, Mann–Whitney U-test; Fig. 8B).

No significant changes were detected under direct exposure to LI 10 J/cm^2 in continuous mode; lacunae and zones of rarefaction of the monolayer appeared only in some places in the reticular growths (Fig. 3A); cells with an increased degree of chromatin compaction (formation of grooves and cords of various shapes and sizes in the nucleus, located on the periphery), "bare" nuclei were

observed (Fig. 3C). Under the same conditions in the pulse mode, wide lacunae and devastation in the reticular growth zone, cells at different stages of degeneration (giant and pyknotized, with reduced cytoplasm, vacuoles of various sizes, "bare" nuclei) were detected. The whole spectrum of destructive changes was observed in the cell nuclei: a high degree of atypia, protrusions, condensation of chromatin in the form of pits and cords around the karyolem, intranuclear vacuoles, karyopyknosis and karyolysis (Fig. 3C).

With an increased dose of LI up to 25 J/cm^2 in continuous mode, partial destruction of the growth zone with the appearance of large areas of devastation, an increase in the number of degenerate round-shaped cells without appendages (Fig. 3A), with signs of lysis and complete reduction of cytoplasm ("bare" nuclei) were observed; in less damaged areas, the cells had vacuoles in the cytoplasm and perinuclear devastation, nuclei with protrusions, marginal condensation of chromatin, in a state of pyknosis and karyolysis. Giant cells with vacuolated nuclei appeared (Fig. 3C). Under the same conditions, in the pulse mode, deepening of destruction processes was observed: the growth zone disintegrated into small fragments of the reticulum and individual cells. Giant cells with vacuolated nuclei and perinuclear devastation, vacuoles of various sizes in the cytoplasm, as well as compacted cytoplasm, "bare" nuclei were detected. The nuclei of the cells were marked by atypia, had deep condensation of chromatin or were in a state of karyopyknosis.

Under the combined effect of chlorine E6 and LI 10 J/cm^2 in a continuous mode, a reduction of the growth zone, retraction of cells with the formation of large areas of devastation occurred (Fig. 3A). "Bare" nuclei, cells with compacted and reduced cytoplasm and pyknotic nuclei, giant forms of cells with vacuolated nuclei, anucleated cells were found in the fragments of the growth zone. Under the same conditions, in the pulse mode, further destruction of the growth zone was observed. All cultured cells had membrane disturbances, anucleated cells and "naked" nuclei, cells with pyknotized nuclei and nuclei in a state of karyolysis were detected (Fig. 3C).

Under the combined effect of chlorine E6 and LI of a larger dose of 25 J/cm^2 in a continuous mode, almost complete destruction of the reticular growth zone was observed; giant forms of cells with compacted cytoplasm or huge vacuoles, nuclei containing vacuoles, in a state of karyopyknosis and karyolysis, a large number of anucleate cells were detected. Under the same conditions in the pulse mode, total destruction of the growth zone was observed (the number of cells decreased by 1.7 times, $p = 0.02$, compared to the control, Mann–Whitney U-test), necrobiotic changes in cells, anucleated and pyknotized cells, "naked" nuclei were detected (Fig. 3, A, C).

The mitotic activity of GB cells decreased under the influence of experimental factors, starting with incubation with chlorine E6 ($p = 0.25$) and reaching a significant decrease under the influence of LI 25 J/cm^2 in pulse mode ($p = 0.015$) and practically leveling off under the combined influence of chlorine E6 and LI in all applied modes ($p = 0.015$ compared to the control, Mann–Whitney U-test; Fig. 8B). In the process of changing the research factors from direct exposure to chlorine E6 or LI to their combined influence, the complete destruction of the growth zone in GB cell culture occurred under the conditions of combined exposure to chlorine E6 and a dose of LI 25 J/cm^2 in pulse mode (under these conditions, the number of tumor cells in culture decreased by 1.7 times, mitotic activity was not detected).

Gliosarcoma (CNS WHO grade G4) cell cultures. Control cell cultures reached confluent growth on the 18th day: the reticular growth zone of stromal component was formed by intercellular connections of cells with stellate, triangular cytoplasm and several branched processes, marked atypia (polymorphism of nuclei and nucleoli); there were also cells of the neuroepithelial type with a wide spread cytoplasm (Fig. 4, A–C). MI was (0.34 ± 0.07) % (Fig. 8C), which is lower than the indicator of GB cells ($p = 0.19$, Mann–Whitney U-test).

After 24 h of incubation with chlorine E6, retraction of the growth zone with its partial destruction and disintegration into fragments, residual complexes and individual cells (Fig. 4A) at various stages of degeneration was revealed: reduction, vacuolization of the cytoplasm, perinuclear devastation, "bare" nuclei, "ring-shaped" cells; nuclei with high atypia, in a state of karyopyknosis and karyorhexis, with protrusions and deep or severe condensation of chromatin (Fig. 4C). No mitotically active cells were detected.

Under the direct influence of LI 10 J/cm^2 in a continuous mode, the retraction of the growth zone with the formation of large lacunae between the fragments of the monolayer of the reticular structure was noted; vacuolar dystrophy of a part of cells and atypia of nuclei (legume, flattened, with membranes); compaction of chromatin in the form of grooves and strands around the karyolem were

detected (Fig. 4, A, C). Under the same conditions, in the pulsed mode, destruction of the growth zone, total accumulation of TB by cells, cells with cytoplasmic vacuolization and perinuclear devastation ("ring-shaped" cells), dark and homogeneous nuclei were observed. MI under the influence of LI of this dose was kept at the level of (0.29–0.18)% (Fig. 8C).

Under the influence of LI at a higher dose of 25 J/cm^2, further destruction of the growth zone and cell alterations were observed continuously: from cytoplasm compaction to its vacuolization, from chromatin compaction in the nuclei to their pyknotization. Under the same conditions in pulse mode, small fragments of reticulum remnants, individual cells with and without appendages were observed. Cytoplasm reduction was determined in cells with preserved appendages, which later led to the appearance of "bare" nuclei. Some of the cells in the cytoplasm had vesicles, vacuoles of various sizes and perinuclear devastation. Nuclei were characterized by atypia in size and shape, with protrusions and an increase in the degree of chromatin condensation in the form of globs or cords of various shapes and sizes (Fig. 4, A, C). No cells in the state of mitotic division were detected.

Under the combined effect of chlorine E6 and LI 10 J/cm^2 in a continuous mode, widespread destruction of the growth zone was observed. In the remaining fragments of the reticulum, cells with rounded cytoplasm and completely or partially reduced appendages, "bare" nuclei, cells with large perinuclear devastation ("annular" cells) were found; most nuclei are in a state of pyknosis or with compaction of chromatin in the form of strands and globs; anucleate cells. Under the same conditions in the pulse mode, the disintegration of the growth zone into small fragments was noted; degenerative manifestations in cells with subsequent necrotization (partial or complete reduction of processes, cytoplasm compaction, vacuolization and perinuclear devastation, nuclear pyknosis; "bare" nuclei were observed (Fig. 4, A, C).

Under the combined effect of chlorine E6 and LI of a larger dose of 25 J/cm^2 in a continuous mode, a destroyed growth zone; rather large single fragments of the reticulum, with cells with large cytoplasm of various shapes, large rounded light nuclei and long winding processes were observed. The main mass of cells had irreversible necrotic changes (condensation, reduction of cytoplasm, "bare" nuclei; flattening or shrinkage of the nucleus, atypical nuclei with chromatin condensation, karyopyknosis with signs of autophagy). Under the same conditions, in the pulse mode, complete destruction of the growth zone was noted, cells at various stages of degeneration (condensed, homogenized cytoplasm with signs of cytolysis and reduction, "bare" nuclei; wrinkled hyperchromic nuclei of cells in a state of pyknosis) (Fig. 4, A, C).

According to quantitative studies, under the influence of experimental factors, the total number of cells in the gliosarcoma culture and their mitotic activity gradually decreased (Fig. 8C). In the process of changing the research factors from direct exposure to chlorine E6 or LI to their combined influence, there was a gradual increase in cytodestructive effects in gliosarcoma cell culture, reaching a total character under the conditions of combined exposure to chlorine E6 and a dose of LI 25 J/cm^2 in pulse mode (under these conditions, the number of cells in the culture decreased by 4.2 times ($p = 0.0002$ compared to the control, Mann–Whitney U-test), mitotic activity was not detected).

Astrocytoma (CNS WHO grade G3, continued growth) cell cultures. Cultures of recurrent astrocytoma cells, reached confluent growth on the 18th day: large arrays of monolayer growths of fibroblast-like cells, closely adjacent to each other, with centrally located light, round or oval-shaped nuclei, and several tortuous processes (Fig. 5, A, C). MI was (0.20 ± 0.07)% (Fig. 8D), which is comparable to the indicator of primary astrocytoma cells ($p = 0.92$, Mann–Whitney U-test).

After 24 h of incubation with chlorine E6, significant destruction of the dense monolayer of the growth zone, dystrophic changes in part of the cells (reduction of processes and rounding of the cytoplasm, its vacuolization; pyknosis of the nuclei (shrinkage, decrease in volume, hyperchromia), their vacuolization (such nuclei remained pale, irregular shape, with deep compaction of chromatin), perinuclear devastation, which sometimes changed the shape of the cells to "annular", were detected. The most typical change in the cytoplasm was its complete reduction, which led to the appearance of "naked" nuclei (Fig. 5, A, C). MI was at a low level (Fig. 8D).

Under direct exposure to LI 10 J/cm^2 in a continuous mode, ruptures of the monolayer growth zone and disintegration into separate clusters of cells with compacted cytoplasm or small vacuoles, "bare" nuclei were observed. Cell nuclei were atypical, different in size and shape (bean-shaped, triangular, crescent), had perinuclear emptying (with the formation of "ring-shaped" cells) and condensation of chromatin in the form of grooves and strands along the periphery of the nucleus up to

karyopyknosis. Under the same conditions, in the pulse mode, destruction of the growth zone, hydropic dystrophy of cells, shift of the nucleus to the periphery, atypia, shrinkage of nuclei, compaction of chromatin, "ring-shaped" cells and "bare" nuclei were noted (Fig. 5, A, C).

Under the influence of LI at a higher dose of 25 J/cm^2 in a continuous mode, the disintegration of the monolayer into separate small fragments and single sprouted cells that were not in contact with each other, with condensed cytoplasm and atypical bean-shaped nuclei were revealed. Cytoplasm vacuolization, perinuclear devastation, marginal chromatin condensation, and pyknotization of nuclei occurred in part of the cells. Under the same conditions, in the pulse mode, retraction of the growth zone with the formation of compacted conglomerates of dystrophically altered tumor cells (reduction, homogenization, vacuolization of the cytoplasm, perinuclear emptying, "ring-shaped" cells, "bare" nuclei; atypical nuclei with vacuoles, chromatin compaction on the periphery) were observed (Fig. 5, A, C).

Under the combined effect of chlorine E6 and LI 10 J/cm^2 in a continuous mode, significant destruction of the growth zone and alteration of cells (typical dystrophic changes) were noted; MI was at a low level (Fig. 8D). Under the same conditions in the pulse mode, complete destruction of the growth zone was observed. In most cells, the cytoplasm was very thin, without clear boundaries, with pyknotic nuclei and perinuclear vacuolization; many "bare" nuclei and nuclei with deep or severe condensation of chromatin were observed (Fig. 5, A, C). Mitotic activity was not detected.

According to quantitative studies, in the process of changing the experimental factors from direct exposure to chlorine E6 or LI to their combined influence, there was a slow increase in cytodestructive effects in the culture of recurrent astrocytoma cells, reaching the greatest manifestation under the conditions of combined exposure to chlorine E6 and a dose of LI 25 J/cm^2 in the pulse mode (under these conditions, the number of cells in the culture decreased by 1.4 times ($p = 0.28$ compared to the control, Mann–Whitney U-test), no mitotic activity was detected).

Oligodendroglioma (CNS WHO grade G3, continued growth) cell cultures. Cultures of recurrent oligodendroglioma cells, reached confluent growth on the 18th day: a monolayer of tumor cells of various sizes with distinct cytoplasm, a large round or oval nucleus, unipolar, triangular, rhomboid, polygonal in shape with appendages of different lengths, and also tightly adjacent to each other one spindle-shaped cell were noted. The formation of intercellular connections with the formation of reticular architecture was detected (Fig. 6, A–C). MI was (0.26 ± 0.08)% (Fig. 8E).

After 24 h of incubation with chlorine E6, deformation and ruptures of the growth zone were detected; cells lost contacts, became isolated, lost processes. Degenerate forms were noted ("fat" cells with hypertrophied cytoplasm); unevenly thinned cytoplasm with vacuolization, perinuclear devastation and areas of cytolysis, atypical nuclei (reduced, flattened, with protrusions, condensation of chromatin on the periphery, pyknosis), "ring-shaped" cells (Fig. 6, A, C). No mitotic activity was detected.

Under direct exposure to LI 10 J/cm^2 in a continuous mode, an increase in the proportion of degenerated cells was observed (reduction of appendages, cytoplasm compaction with increasing homogeneity, "ring-like" shape, nuclear pyknosis, large vacuoles in the perinuclear zone, absence of a nucleus). Under the same conditions, in the pulse mode, large areas of the devastated growth zone and clusters of densely adjacent cells ("syncytia") with necrobiotic changes were observed (a high degree of cytoplasmic vacuolization, plasmalemma defects, atypical nuclear shapes (bean-shaped, triangular, flattened), chromatin condensation around the karyolemma and pyknosis) (Fig. 6, A, C); mitotic activity at a low level (Fig. 8E). Similar changes were also noted under the influence of LI at a higher dose of 25 J/cm^2 in continuous mode and their amplification in pulse mode: significant destruction of the growth zone, the appearance of multinucleated cells, dystrophic and degenerative changes in cells (marginality of chromatin along the intact nuclear membrane, perinuclear vacuoles, pyknotization of nuclei, increase in the number of cytoplasmic vacuoles, membrane wear), leveling of mitotic activity.

Under the combined effect of chlorine E6 and LI 10 J/cm^2 in a continuous mode, a significant deformation of the growth zone, mostly degenerated cells (reduction of processes, membrane wear, vacuolization of the cytoplasm with perinuclear devastation, nuclei in various stages of destruction) were observed. Under the same conditions in the pulse mode, destructive changes increased: multinucleated cells with condensed cytoplasm and flattened nuclei, cytoplasmic vacuoles, membrane wear, perinuclear emptying and "shadow" cells without nuclei were noted (Fig. 6, A, C). No mitotic activity was detected.

Under the combined effect of chlorine E6 and LI 25 J/cm^2 in a continuous mode, the growth zone disintegrated into small islands of a monolayer structure and a reticular structure. In the cytoplasm of most cells, vacuolization and perinuclear devastation were noted; some nuclei are reduced, some are flattened, some nuclei are pyknotic and with perinuclear vacuoles. Under the same conditions in the pulse mode, the growth zone was disintegrated, the small number of remaining cells were dystrophically altered (atypical nuclei at various stages of destruction, perinuclear vacuoles, chromatin condensation, pyknosis, karyolysis; vacuolated cytoplasm) (Fig. 6, A, C). No mitotic activity was detected.

According to quantitative studies, in the process of changing the experimental factors from direct exposure to chlorine E6 or LI to their combined influence, there was a gradual increase in cytodestructive effects in recurrent oligodendroglioma cell culture, reaching the greatest manifestation under the conditions of combined exposure to chlorine E6 and a dose of LI 25 J/cm^2 in the pulse mode (under these conditions, the number of cells in the culture was halved ($p = 0.01$ compared to the control, Mann–Whitney U-test), no mitotic activity was detected). It is possible that for the total destruction of tumor cells it is necessary to use an increased dose of LI or a repeated session of the same dose of LI.

GB (CNS WHO grade G4, continued growth) cell cultures. Cultures of recurrent GB cells, reached confluent growth on the 26th day: reticular growths of cells with developed cytoplasm, round or oval nuclei, long, thick and very branched tortuous processes (Fig. 7, A–C). MI reached an average of (0.57 ± 0.05)% (Fig. 8F).

After 24 h of incubation with chlorine E6, cells with shorter and fewer processes and granules of TB in the condensed cytoplasm, atypical nuclei were detected (Fig. 7, A–C). Mitotic activity leveled off ($p = 0.047$ compared to the control, Mann–Whitney U-test; Fig. 8F).

Under direct exposure to LI 10 J/cm^2 in a continuous mode, no significant changes in the structure and histoarchitectonics of the growth zone were detected. TB in the form of grains was concentrated in the cytoplasm of cells that did not lose their morphology, and completely stained the degenerated cells of a rounded shape with reduced processes. Among the cells with long winding processes, "bare" nuclei, cells with nuclear atypia (flattened shape, bean-shaped, with blades), perinuclear vacuoles, pyknosis, "ring-shaped" forms were observed (Fig. 7, A, C). Under the same conditions in the pulse mode, local destruction of the monolayer of cells, accumulation of vital dye by all cells was observed, among the small number of cells with preserved morphology, cells with various damages were distinguished.

Under the influence of LI with a higher dose of 25 J/cm^2 in a continuous mode, areas with a completely destroyed structure were observed along with intact areas of the growth zone; cells with a sharp reduction of cytoplasm, pyknotic nuclei, without appendages or with the loss of a significant number of them, "bare" nuclei, "shadow" cells (Fig. 7, A, C). Under the same conditions, in pulse mode, the disintegration of the growth zone into separate fragments of the reticular structure was observed, between which there were areas of devastation with single proliferative cells, condensed cytoplasm, with large perinuclear vacuoles, atypical nuclei of various sizes and shapes, mostly pyknotized.

Under the combined effect of chlorine E6 and LI 10 J/cm^2 in a continuous mode, destruction of the growth zone was detected, only in some areas cells with tortuous processes were observed, most of the cells were in various stages of degeneration (reduction of cytoplasm, "bare" nuclei, perinuclear vacuoles, heavy condensation of chromatin around cariolem, pyknosis). Under the same conditions, similar changes were observed in the pulse mode (Fig. 7, A, C).

Under the combined effect of chlorine E6 and LI of a higher dose of 25 J/cm^2 in a continuous mode, a destroyed growth zone and residual islands of cells with tortuous processes, perinuclear devastation and pyknotic nuclei, "bare" nuclei and anucleate cells were observed; the same changes were observed in the pulse mode (Fig. 7, A, C).

According to quantitative studies, in the process of changing the research factors from direct exposure to chlorine E6 or LI to their combined influence, there was a gradual increase in cytodestructive effects in recurrent GB cell culture, reaching the greatest manifestation under the conditions of combined exposure to chlorine E6 and a dose of LI 25 J/cm^2, and the degree of destruction was comparable for continuous and pulse modes (under these conditions, the number of cells in the culture decreased by 2.3 times ($p = 0.001$ compared to the control, Mann–Whitney U-test), mitotic activity was not detected).

Discussion

PDT is considered a promising adjuvant method of MG treatment, including with tumor relapses [7, 13–19]. Clinical studies use stereotaxic PDT in primary (NCT03897491) and recurrent (NCT04469699) GB, as well as intraoperative and interstitial PDT (iPDT) in primary GB (NCT04391062, NCT03897491) [30].

For the clinical application of PDT, it is important to choose effective and optimal doses of LI and PS. An adequate tool for selecting such doses can be primary cultures of MG cells obtained directly from tumor tissue.

The relevance and expediency of determining individual personalized doses of LI and PS for PDT is confirmed in our study by the unequal growth dynamics of primary cultures of MG cells: depending on the individual characteristics of the tumor, tumor cell cultures formed a confluent monolayer from the 18th to the 25th day of cultivation. At the same time, the mitotic activity of tumor cells varied, as expected, from the highest index of MI in the culture of primary GB to lower – in cultures of recurrent GB (p = 0.45), and cultures of primary astrocytoma and gliosarcoma (p = 0.03, p = 0.19) – and the smallest - in cultures of recurrent astrocytoma and oligodendroglioma (p = 0.01, p = 0.24, compared to the indicator of primary GB cells, Mann–Whitney U-test).

Chlorine E6, which is considered one of the most effective modern PS [10, 23, 25–27], accumulated in the cytoplasm of tumor cells; fluorescence intensity varied between different histological cell types. We used a PS concentration of 2 μg/ml based on the results of previous studies, in which this dose was found to be optimal for the cytodestructive photodynamic effect on human GB cells of the U251 line [29]. Direct exposure to chlorine E6 was characterized by a certain degree of cytodestructive effects in MG cell cultures, reducing the mitotic activity of tumor cells or completely eliminating it in cases of primary astrocytoma and gliosarcoma, recurrent oligodendroglioma and GB (significant in the case of recurrent GB, p = 0.047, compared to control, Mann–Whitney U-test). In the following studies, it is probably advisable to use a higher concentration of PS as well.

The direct influence of LI (λ = 650 nm, power 0.6 W, dose 10 and 25 J/cm^2) was also characterized by a certain degree of cytodestructive effects in the cultures of MG cells, reducing the total number of cells in the culture and their mitotic activity. Increasing the LI dose from 10 to 25 J/cm^2 in a continuous mode consistently led to destructive changes in the architecture of the growth zone (from the retraction of the growth zone with the formation of lacunae of various sizes at lower LI indicators to the gross destruction of architecture and significant devastation of cell arrays at higher indicators). A decrease in the mitotic activity of tumor cells and the accumulation of necrobiotic changes in them up to irreversible degeneration with subsequent desquamation of dead cells were also found. Such an effect had a tendency to increase with the same LI characteristics in the pulse mode. The greatest effect was expected to be achieved with the combined effect of chlorine E6 and LI.

Cytodestructive effects in MG cell cultures were evaluated by a set of indicators: qualitative (a decrease in the level of cellular metabolism according to the degree of damage to the nucleus and disruption of the karyolem, from signs of early destruction of the nucleus (an increase in the number of vacuolated and hyperchromic nuclei), compaction of chromatin, perinuclear devastation before its completion (karyopyknosis, karyorrhexis, karyolysis); degree of reduction of appendages and cytoplasm, vacuolization, disruption of plasmalemma) and quantitative (dynamics of changes in the total number of cells in the culture and their mitotic activity).

As a result of the conducted morphological and morphometric study, it was established that under the combined effect of chlorine E6 (2 μg/ml) and LI (0.6 W), the effective dose in the case of primary astrocytoma cells is 10 J/cm^2 in pulse mode; for cells of primary GB, primary gliosarcoma, recurrent astrocytoma, and recurrent oligodendroglioma, the effective dose is 25 J/cm^2 in pulsed mode. In the case of GB cells, continued growth, the dose efficiency of 25 J/cm^2 is comparable for continuous and pulsed modes. Under the indicated conditions, the combined effect of chlorine E6 (2 μg/ml) and LI (0.6 W) achieved the most pronounced destruction of the growth zone in MG cell cultures, a significant decrease in the number of cells, cessation of mitotic activity. The specified modes of photodynamic exposure did not have a similar destructive effect on cultures of non-malignant cells (cultures of reference cells HEK293) [31].

To understand the mechanisms of the antitumor effects of PDT, it is necessary to refer to the principles of the method, which is based on cytotoxic effects caused by a cascade of molecular

events. PDT involves 2 stages: 1) the introduction of a light-sensitive chemical agent (PS); 2) its activation at a certain wavelength of light. Activation of PS, selectively accumulated in neoplasm cells, by light rays of the appropriate wavelength [32, 33], leads to exciting PS from its ground state (PS) to a singlet excited state (^{1}PS), followed by intersystem crossing to a long-lived triplet excited state (^{3}PS) [8]. The interaction of triplet excited ^{3}PS with ground state (triplet) oxygen ($^3O_2$) or some electron/hydrogen donor leads to the reactive oxygen species (ROS) generation such as singlet molecular oxygen ($^1O_2$) or free radicals (hydrogen peroxide (O_2H), superoxide radical (O_2^-), hydroxyl radical (OH·)) and initiation of a cascade of biochemical events [8, 34–36]. Singlet oxygen ($^1O_2$) is a key ROS responsible for photodynamic damage, despite the limited time of life [37]. $^1O_2$ and other ROS react rapidly with macromolecules containing unsaturated double bonds (proteins, unsaturated fatty acids, cholesterols), damaging the membranes of intracellular organelles (mitochondria, lysosomes, endoplasmic reticulum), reacting with DNA, proteins, lipids and other macromolecules, disrupt multiple cell signaling pathways, extensively destroy DNA, which eventually leads to tumor cells death (through necrosis, apoptosis, autophagy) [8, 32, 35, 36, 38–40]. In this connection, the question of the selectivity of inclusion of PS in tumor cells is important. The tumor tissue is believed to have a higher affinity for the PS, which selectively incorporates into neoplasm cells [32]. It is related to: 1) the higher metabolism level of MG tumor cells compared to non-transformed cells [41, 42], as well as their faster accumulation of the PS compared to normal cells; 2) the low pH levels of tumor tissue due to excess lactic acid production during active glycolysis compared to normal cells, because PS dissolve better in acidic environments and consequently accumulate more effectively in tumor cells [39, 42]. In our previous study we demonstrated the higher sensitivity of human GB U251 cells to the photodynamic effect of chlorin E6 and LI compared to cells of the non-tumor HEK293 line [31].

Therefore, *in vitro* on the cell level we register the result of direct cytodestructive effect of PDT. On the tissue and organism level the PDT leads to destruction of the tumor microvascular system, local ischemia, as well as to activation of antitumor immune responses [8, 32, 38, 39, 44]. PDT targets macrophages, which produce inflammatory mediators and cytokines (lymphokines, thromboxanes, prostaglandins, tumor necrosis factor, etc.) after PDT, thus significantly affecting the tumor stroma degradation; PDT damages endothelial cells, which leads to local thrombosis, vasoconstriction and ultimately to the destruction of the microcirculatory channel. The combination of these effects induces a strong immune response against glioma in the experiment [38]. Therefore, *in vivo* PDT engages the mechanisms of not only direct cytodestructive, but also mediated immunomodulatory antitumor effects, activating the links of innate and acquired immunity.

Concerning potential for translating the obtained *in vitro* results into clinical practice it should be noted that PDT as a treatment method has a clearly focused effect aimed at selectively increasing the zone of tumor destruction during surgery. The simultaneous use of fluorescence-guided surgery and PDT allows for the visualization and targeted destruction of tumor cells [8, 32], optimizing the determination of tumor spreading boundaries for maximal removal [45]. Individual selection of optimal doses and regimes of PDT for a specific patient using the primary cultures *in vitro* will contribute to improving the survival time and quality of life of patients with MG and also provide benefits such as high efficiency, organ-preserving technology and low systemic toxicity.

Conclusions

Primary cultures of MG cells obtained directly from tumor tissue are an adequate tool for evaluating the effectiveness of the cytodestructive effect of the combined use of LI and PS for the clinical application of photodynamic exposure technologies.

In our study on primary MG cell cultures the effective cytodestructive effect of combined use of chlorine E6 (2 μg/ml) and LI (0.6 W) have been established: in the case of primary diffuse astrocytoma cells – when 10 J/cm^2 in pulse mode applied; for cells of primary GB, primary gliosarcoma, recurrent astrocytoma, and recurrent oligodendroglioma, – when LI 25 J/cm^2 in pulse mode applied. In the case of recurrent GB cells, the effective cytodestructive effect have been achieved when LI 25 J/cm^2 applied both in continuous and pulse modes.

In the future studies, it is expedient also to use a higher concentration of PS as wel as an increased dose of LI or a repeated session of the same dose of LI.

Interests disclosure

The authors have no conflict of interest to declare.

The research was conducted without sponsorship.

The study is part of a research work (state registration number 0122U000331).

References

[1] Fedorenko Z, Goulak L, Gorokh Y, Ryzhov A, Soumkina O. Cancer in Ukraine, 2021-2022: Incidence, mortality, prevalence and other relevant statistics [Bulletin of the National Cancer Registry of Ukraine, vol. 24]. National Cancer Registry of Ukraine; 2023. Available at: http://ncru.inf.ua/publications/BULL_24/PDF_E/bull_eng_24.pdf

[2] Low JT, Ostrom QT, Cioffi G, Neff C, Waite KA, Kruchko C, et al. Primary brain and other central nervous system tumors in the United States (2014-2018): A summary of the CBTRUS statistical report for clinicians. Neurooncol Pract. 2022 Feb 22;9(3):165-82. DOI: 10.1093/nop/npac015

[3] Louis DN, Perry A, Wesseling P, Brat DJ, Cree IA, Figarella-Branger D, et al. The 2021 WHO Classification of Tumors of the Central Nervous System: a summary. Neuro Oncol. 2021; Aug 2;23(8):1231-51. DOI: 10.1093/neuonc/noab106

[4] Ostrom QT, Price M, Neff C, Cioffi G, Waite KA, Kruchko C, et al. CBTRUS Statistical Report: Primary brain and other central nervous system tumors diagnosed in the United States in 2016–2020. Neuro Oncol. 2023 Oct 4;25(12 Suppl 2):iv1-iv99. DOI: 10.1093/neuonc/noad149

[5] Dupont C, Vermandel M, Leroy HA, Quidet M, Lecomte F, Delhem N, et al. Intraoperative photodynamic therapy for glioblastomas (INDYGO): Study protocol for a Phase I clinical trial. Neurosurgery. 2019 Jun 1;84(6):E414-9. DOI: 10.1093/neuros/nyy324

[6] van Solinge TS, Nieland L, Chiocca EA, Broekman MLD. Advances in local therapy for glioblastoma - taking the fight to the tumour. Nat Rev Neurol. 2022;Apr;18(4):221-36. DOI: 10.1038/s41582-022-00621-0

[7] Muragaki Y, Akimoto J, Maruyama T, Iseki H, Ikuta S, Nitta M, et al. Phase II clinical study on intraoperative photodynamic therapy with talaporfin sodium and semiconductor laser in patients with malignant brain tumors. J Neurosurg. 2013 Oct;119(4):845-52. DOI: 10.3171/2013.7.JNS13415

[8] Quirk BJ, Brandal G, Donlon S, Vera JC, Mang TS, Foy AB, et al. Photodynamic therapy (PDT) for malignant brain tumors--where do we stand? Photodiagnosis Photodyn Ther. 2015 Sep;12(3):530-44. DOI: 10.1016/j.pdpdt.2015.04.009

[9] Abdel Gaber SA, Müller P, Zimmermann W, Hьttenberger D, Wittig R, Abdel Kader MH, et al. ABCG2-mediated suppression of chlorin e6 accumulation and photodynamic therapy efficiency in glioblastoma cell lines can be reversed by KO143. J Photochem Photobiol B. 2018 Jan;178:182-91. DOI: 10.1016/j.jphotobiol.2017.10.035

[10] Domka W, Bartusik-Aebisher D, Rudy I, Dynarowicz K, Pięta K, Aebisher D. Photodynamic therapy in brain cancer: mechanisms, clinical and preclinical studies and therapeutic challenges. Front Chem. 2023;11:1250621. DOI: 10.3389/fchem.2023.1250621

[11] Hsia T, Small JL, Yekula A, Batool SM, Escobedo AK, Ekanayake E, et al. Systematic review of photodynamic therapy in gliomas. Cancers. 2023;15(15):3918. DOI: 10.3390/cancers15153918

[12] Aebisher D, Przygórzewska A, Myśliwiec A, Dynarowicz K, Krupka-Olek M, Bożek A, et al. Current photodynamic therapy for glioma treatment: An update. Biomedicines. 2024;12(2):375. DOI: 10.3390/biomedicines12020375

[13] van Linde ME, Brahm CG, de Witt Hamer PC, Reijneveld JC, Bruynzeel AME, Vandertop WP, et al. Treatment outcome of patients with recurrent glioblastoma multiforme: a retrospective multicenter analysis. J Neurooncol. 2017;Oct;135(1):183-92. DOI: 10.1007/s11060-017-2564-z

[14] Schipmann S, Müther M, Stögbauer L, Zimmer S, Brokinkel B, Holling M, et al. Combination of ALA-induced fluorescence-guided resection and intraoperative open photodynamic therapy for recurrent glioblastoma: case series on a promising dual strategy for local tumor control. J Neurosurg. 2020 Jan 24;134(2):426-36. DOI: 10.3171/2019.11.JNS192443

[15] Lietke S, Schmutzer M, Schwartz C, Weller J, Siller S, Aumiller M, et al. Interstitial photodynamic therapy using 5-ALA for malignant glioma recurrences. Cancers (Basel). 2021 Apr 7;13(8):1767. DOI: 10.3390/cancers13081767

[16] Vermandel M, Dupont C, Lecomte F, Leroy HA, Tuleasca C, Mordon S, et al. Standardized intraoperative 5-ALA photodynamic therapy for newly diagnosed glioblastoma patients: a preliminary analysis of the INDYGO clinical trial. J Neurooncol. 2021 May;152(3):501-14. DOI: 10.1007/s11060-021-03718-6

[17] Kobayashi T, Nitta M, Shimizu K, Saito T, Tsuzuki S, Fukui A, et al. Therapeutic options for recurrent glioblastoma-efficacy of talaporfin sodium mediated photodynamic therapy. Pharmaceutics. 2022;14(2):353. DOI: 10.3390/pharmaceutics14020353

[18] Vilchez ML, Rodríguez LB, Palacios RE, Prucca CG, Caverzán MD, Caputto BL, et al. Isolation and initial characterization of human glioblastoma cells resistant to photodynamic therapy. Photodiagnosis Photodyn Ther. 2021 Mar;33:102097. DOI: 10.1016/j.pdpdt.2020.102097

[19] Ren Z, Wen J, Mo Y, Zhang P, Chen H, Wen J. A systematic review and meta-analysis of fluorescent-guided resection and therapy-based photodynamics on the survival of patients with glioma. Lasers Med Sci. 2022 Mar;37(2):789-97. DOI: 10.1007/s10103-021-03426-7

[20] Santos KLM, Barros RM, da Silva Lima DP, Nunes AMA, Sato MR, Faccio R, et al. Prospective application of phthalocyanines in the photodynamic therapy against microorganisms and tumor cells: A mini-review. Photodiagnosis Photodyn Ther. 2020 Dec;32:102032. DOI: 10.1016/j.pdpdt.2020.102032

[21] Leroy HA, Guérin L, Lecomte F, Baert G, Vignion AS, Mordon S, et al. Is interstitial photodynamic therapy for brain tumors ready for clinical practice? A systematic review. Photodiagnosis Photodyn Ther. 2021;36:102492. DOI: 10.1016/j.pdpdt.2021.102492

[22] Bartusik-Aebisher D, Żołyniak A, Barnaś E, Machorowska-Pieniążek A, Oleś P, Kawczyk-Krupka A, et al. The use of photodynamic therapy in the treatment of brain tumors—A review of the literature. Molecules. 2022;27(20):6847. DOI: 10.3390/molecules27206847

[23] PubChem. Bethesda (MD): National Library of Medicine (US), National Center for Biotechnology Information; 2004-. PubChem Compound Summary for CID 5479494, Chlorin e6.

[24] Shrestha R, Lee HJ, Lim J, Gurung P, Thapa Magar TB, Kim YT, et al. Effect of photodynamic therapy with chlorin e6 on canine tumors. Life. 2022;12(12):2102. DOI: 10.3390/life12122102

[25] Thapa Magar TB, Mallik SK, Gurung P, Lim J, Kim YT, Shrestha R, et al. Chlorin E6-curcumin-mediated photodynamic therapy promotes an anti-photoaging effect in UVB-irradiated fibroblasts. Int J Mol Sci. 2023 Aug 30;24(17):13468. DOI: 10.3390/ijms241713468

[26] Hur GH, Ryu AR, Kim YW, Lee MY. The potential anti-photoaging effect of photodynamic therapy using chlorin e6-curcumin conjugate in UVB-irradiated fibroblasts and hairless mice. Pharmaceutics. 2022;14(5):968. DOI: 10.3390/pharmaceutics14050968

[27] Hak A, Ali MS, Sankaranarayanan SA, Shinde VR, Rengan AK. Chlorin e6: a promising photosensitizer in photo-based cancer nanomedicine. ACS Appl Bio Mater. 2023;6(2):349-64. DOI: 10.1021/acsabm.2c00891

[28] Hamaliya MF, Shyshko YD, Shton' IO, Kholin VV, Shcherbakov OB, Usatenko OV. [Photodynamic activity of second-generation photosensitizer fotolon (chlorin e6) and its golden nanocomposite: experiments in vitro and in vivo]. Photobiol Photomed. 2012;9(1-2):99-103.

[29] Rozumenko VD, Liubich LD, Staino LP, Egorova DM, Vaslovych VV, Rozumenko AV, et al. Effects of photodynamic exposure using chlorine E6 on U251 glioblastoma cell line in vitro. Ukr Neurosurg J. 2023;29(2):11-21. DOI: 10.25305/unj.273699

[30] Search of: photodynamic therapy | Glioma - List Results [Internet]. U.S. National Library of Medicine. ClinicalTrials.gov [Cited 2024 Sept 25]. Available at: https://clinicaltrials.gov/ct2/results?cond=Glioma&term=photodynamic++therapy&cntry=&state=&city=&dist=&Search=Search

[31] Rozumenko VD, Liubich LD, Staino LP, Egorova DM, Dashchakovskyi AV, Vaslovych VV, et al. Comparison of the effects of photodynamic exposure with the use of chlorine E6 on glioblastoma cells of the U251 line and human embryonic kidney cells of the HEK293 line in vitro. Ukr Neurosurg J. 2024;30(3):38-51. DOI: 10.25305/unj.306363

[32] Cramer SW, Chen CC. Photodynamic therapy for the treatment of glioblastoma. Front Surg. 2020;6:81. DOI: 10.3389/fsurg.2019.00081

[33] Dubey SK, Pradyuth SK, Saha RN, Singhvi G, Alexander A, Agrawal M, et al. Application of photodynamic therapy drugs for management of glioma. J Porphyrins Phthalocyanines. 2019;23(11n12):1216-28. DOI: 10.1142/S1088424619300192

[34] Sobhani N, Samadani AA. Implications of photodynamic cancer therapy: an overview of PDT mechanisms basically and practically. J Egypt Natl Canc Inst. 2021;33:34. DOI: 10.1186/s43046-021-00093-1

[35] Maharjan PS, Bhattarai HK. Singlet oxygen, photodynamic therapy, and mechanisms of cancer cell death. J Oncol. 2022 Jun 25;2022:7211485. DOI: 10.1155/2022/7211485

[36] Przygoda M, Bartusik-Aebisher D, Dynarowicz K, Cieślar G, Kawczyk-Krupka A, Aebisher D. Cellular mechanisms of singlet oxygen in photodynamic therapy. Int J Mol Sci. 2023;24:16890. DOI: 10.3390/ijms242316890

[37] Szewczyk G, Mokrzyński K, Sarna T. Generation of singlet oxygen inside living cells: correlation between phosphorescence decay lifetime, localization and outcome of photodynamic action. Photochem Photobiol Sci. 2024;23:1673-85. DOI: 10.1007/s43630-024-00620-8

[38] Li F, Cheng Y, Lu J, Hu R, Wan Q, Feng H. Photodynamic therapy boosts anti-glioma immunity in mice: a dependence on the activities of T cells and complement C3. J Cell Biochem. 2011;112(10):3035-43. DOI: 10.1002/jcb.23228

[39] Kaneko S, Fujimoto S, Yamaguchi H, Yamauchi T, Yoshimoto T, Tokuda K. Photodynamic therapy of malignant gliomas. Prog Neurol Surg. 2018;32:1-13. DOI: 10.1159/000469675

[40] Yanovsky RL, Bartenstein DW, Rogers GS, Isakoff SJ, Chen ST. Photodynamic therapy for solid tumors: a review of the literature. Photodermatol Photoimmunol Photomed. 2019;35(5):295-303. DOI: 10.1111/phpp.12489

[41] Márquez J, Alonso FJ, Matés JM, Segura JA, Martín-Rufián M, Campos-Sandoval JA. Glutamine addiction in gliomas. Neurochem Res. 2017;42(6):1735-46. DOI: 10.1007/s11064-017-2212-1

[42] Rivera JF, Sridharan SV, Nolan JK, Miloro SA, Alam MA, Rickus JL, et al. Real-time characterization of uptake kinetics of glioblastoma vs. astrocytes in 2D cell culture using microelectrode array. Analyst. 2018;143(20):4954-66. DOI: 10.1039/c8an01198b

[43] Moan J, Peng Q. An outline of the history of PDT. In: Patrice T, editor. Photodynamic therapy. London: The Royal Society of Chemistry; 2003. p. 1-18. DOI: 10.1039/9781847551658-00001

[44] Mahmoudi K, Garvey KL, Bouras A, Cramer G, Stepp H, Jesu Raj JG, et al. 5-aminolevulinic acid photodynamic therapy for the treatment of high-grade gliomas. J Neurooncol. 2019;141(3):595-607. DOI: 0.1007/s11060-019-03103-4

[45] Senders JT, Muskens IS, Schnoor R, Karhade AV, Cote DJ, Smith TR, et al. Agents for fluorescence-guided glioma surgery: a systematic review of preclinical and clinical results. Acta Neurochir (Wien). 2017;159(1):151-67. DOI: 10.1007/s00701-016-3028-5

В.Д. Розуменко[1], Л.Д. Любич[2], Л.П. Стайно[2], Д.М. Єгорова[2], А.В. Дащаковський[1], Т.А. Малишева[3]

ЦИТОДЕСТРУКТИВНІ ЕФЕКТИ ФОТОДИНАМІЧНОГО ВПЛИВУ В ПЕРВИННИХ КУЛЬТУРАХ КЛІТИН ЗЛОЯКІСНИХ ГЛІОМ

[1]Відділення інноваційних нейрохірургічних технологій відділу нейроонкології та нейрохірургії дитячого віку, ДУ “Інститут нейрохірургії ім. акад. А.П. Ромоданова Національної академії медичних наук України”, Київ, Україна
[2]Лабораторія культивування тканин відділу нейропатоморфології, ДУ “Інститут нейрохірургії ім. акад. А.П. Ромоданова Національної академії медичних наук України”, Київ, Україна
[3]Патологоанатомічна лабораторія відділу нейропатоморфології, ДУ “Інститут нейрохірургії ім. акад. А.П. Ромоданова Національної академії медичних наук України”, Київ, Україна

Проблематика. Фотодинамічна терапія (ФДТ) є перспективним ад’ювантним методом лікування злоякісних гліом (ЗГ), у т.ч. при продовженому рості та рецидивах пухлин. Для клінічного застосування ФДТ важливо обґрунтувати ефективність цитодеструктивного впливу поєднаного застосування лазерного опромінення (ЛО) і фотосенсибілізатора (ФС).
Мета. Оцінити цитодеструктивні ефекти фотодинамічного впливу із застосуванням ФС хлорину Е6 на первинні культури клітин ЗГ.
Методика реалізації. Первинні культури клітин отримували зі зразків біоптичного матеріалу від пацієнтів (n = 6) з верифікованим діагнозом: 3 первинні пухлини (1 випадок дифузної астроцитоми NOS (G3), 1 – гліобластоми (ГБ) NOS (G4), 1 – гліосаркоми (G4)) і 3 – з продовженим ростом (1 – дифузної астроцитоми NOS (G3), 1 – олігодендрогліоми NOS (G3) та 1 – ГБ NOS (G4). Групи клітинних культур включали: 1) контрольні – культивовані в стандартному живильному середовищі та дослідні, 2) культивовані з додаванням хлорину Е6 (2,0 мкг/мл); 3) культивовані без додавання ФС та піддані ЛО; 4) культивовані з додаванням хлорину Е6 і подальшим впливом ЛО. Через 24 год проводили морфологічні та морфометричні дослідження.
Результати. Первинні культури клітин ЗГ характеризувались неоднаковою динамікою росту; мітотична активність пухлинних клітин варіювала від найвищого показника в культурі первинної ГБ до менших – у культурах рецидивної ГБ і первинних астроцитоми та гліосаркоми – та найменших – у культурі клітин випадків продовженого росту астроцитоми й олігодендрогліоми після комбінованого лікування. Безпосередній вплив хлорину Е6 та ЛО знижував загальну кількість клітин у культурі та їхню мітотичну активність. Найбільшого цитодеструктивного ефекту досягали за поєднаного впливу хлорину Е6 та ЛО: ефективною дозою у випадку клітин первинної астроцитоми є 10 Дж/см^2 в імпульсному режимі; для клітин первинної ГБ та гліосаркоми, рецидивної астроцитоми та олігодендрогліоми ефективною дозою є 25 Дж/см^2 в імпульсному режимі. У випадку клітин ГБ, продовжений ріст, доза 25 Дж/см^2 є ефективною як для безперервного, так і для імпульсного режимів ЛО.
Висновки. Первинні культури клітин ЗГ, отримані безпосередньо з пухлинної тканини, є адекватною моделлю оцінки ефективності цитодеструктивного впливу поєднаного застосування ЛО і ФС для ФДТ.

Ключові слова: злоякісні гліоми; продовжений ріст; первинні культури; фотодинамічна терапія; лазерне опромінення; хлорин Е6; мітотичний індекс.